# Polymer Chemistry

Accepted Manuscript






ROYAL SOCIETY OF CHEMISTRY

www.rsc.org/polymers

Journal Name

RSCPublishing

ARTICLE

# Gradient and Block Side-chain Liquid Crystalline Polyethers

Cite this: DOI: 10.1039/x0xx00000x

Yu Liu, Wei Wei, and Huiming Xiong*

Received ooth January 2012,
Accepted ooth January 2012

DOI: 10.1039/x0xx00000x

www.rsc.org/

A set of gradient copolymers composed of liquid crystalline polyether and poly(butylene oxide) with narrow molecular weight distributions and well-defined, continuous growing composition profiles were synthesized *via* anionic ring-opening polymerization. For comparison, corresponding diblock copolymers without compositional gradient were also prepared. The thermal transitions, phase structures and their evolutions of these two sets of liquid crystalline copolymers with composition and temperature were systematically investigated. The compositional gradient copolymers were found to possess a remarkable sensitivity on the phase structures on multiple length scales. Compared with the corresponding liquid crystalline block copolymers, they exhibited a broad glass transition region and a large breadth of liquid crystalline phase transformation associated with disordered mesogenic packing and a thickness distribution of liquid crystalline layers. Ordered, nanophase separated structures were observed to gradually develop with increase of gradient length. They exhibited distinct ordering and evolution processes with continuous liquid crystalline melting, which are different from the reference samples of diblock copolymers. Those behaviors are speculated to originate from the heterogeneity intrinsic to liquid crystalline gradient copolymer.

## Introduction

Gradient copolymers are a class of binary copolymers with a monotonous gradual distribution of at least two monomeric species (A and B) along polymer chains.[1] In contrast with typical phase segregated diblock copolymers which can form various structures such as lamellae, double gyroids, cylinders and body-centered cubic spheres,[2, 3] continuous variation of monomer concentrations in gradient polymer chains usually leads to a lamellar structure, without distinct points to separate A- and B-rich domains as anticipated in theories.[4-11] Gradient polymers can also serve as a constituting section in different positions of a polymer chain, for instance, to form the so-called tapered-block copolymer.[12-17] Largely widened double gyroid phase regime of diblock copolymer has been predicted when a taper is incorporated into the junction portion of the chain, which has been attributed to the relieved packing frustration due to the gradient nature of the polymer chains.[17]

Recently, extensive experimental works on gradient polymers have been reported in literature.[18-32] With advances in synthetic methodologies such as controlled free radical polymerization techniques, a high degree of precision over the sequence distribution in gradient copolymers has been achieved. This type of copolymers represents one essential way to control the chain architecture that bridges between random copolymers and block copolymers, and is believed to be able to offer opportunities for applications in shock absorption, interfacial modifiers and others.[23, 24] So far, the gradient copolymers usually encompass conventional monomers and the report on gradient polymers incorporated with functional monomers is rather limited.[20, 28] In this article, we describe a novel class of liquid crystalline gradient polyether with a narrow molecular weight distribution synthesized through a living anionic ring-opening polymerization in a convenient, batch mode.

Liquid crystalline random copolymers have been investigated extensively, typically synthesized *via* free radical polymerization.[33, 34] However, the study of gradient liquid crystalline copolymer has not been reported to our best knowledge. In merits of our successful synthesis of liquid crystalline homopolymer by controlled anionic polymerization previously,[35-37] design of liquid crystalline gradient copolymers becomes feasible. The resulting copolymers with gradient distributions of co-monomers could possess narrow molecular weight distributions compared to those obtained *via* conventional free radical polymerizations.[33, 34, 38, 39] On another aspect, the unique gradient feature of the polymer chains is expected to generate unusual structures and properties such as novel thermal behaviors.[19, 40, 41] It is thus particularly interesting to explore how the chain architecture in liquid crystalline field would affect their phase structures on different length scales and to investigate the structure-property relationships of this new type of copolymers.

Herein, we report for the first time on the synthesis and characterization of a series of liquid crystalline gradient and block copolymers in different liquid crystalline compositions with respect to poly(butylene oxide) (PBO) component. The effects of continuous compositional sequence changes on liquid

crystalline phase behaviors and nano-structures have been investigated. Interestingly, the gradient copolymers are found to form ordered nanophase separated structures even for the smooth gradient composition profiles. They exhibit distinct thermal phase behaviors and structure evolutions from the block copolymers. The gradient nature of those polymer backbones coupled with liquid crystalline field is further discussed.

## Experimental section

### Materials

Toluene was stirred with sodium over 24 h and distilled into a high-vacuum flask which was flame-dried three times, and freeze-thawed three times in a vacuum line. 18-crown-6, potassium *tert*-butoxide (Acros Organics) in a concentration of 1M in tetrahydrofuran (THF) and dibutylmagnesium (Acros Organics) were all used as received. Liquid crystal monomer was synthesized as previously reported.[36]

### Synthesis of gradient copolymers

The anionic ring-opening polymerization of epoxide monomers follows the procedure developed for non-mesogenic monomers,[42] which was adapted to the synthesis of liquid crystalline polyethers.[35-37] Briefly, a high-vacuum reactor flask containing a stir bar was placed in a high-vacuum line and flame-dried three times. The liquid crystalline monomers (0.5 g, 1.34 mmol) were added into the flask and degassed at 40 °C. 18-crown-6 (14 mg, 50 umol) was then added into the reactor flask under the nitrogen atmosphere and vacuumed thereafter. Benzene was distilled into the reactor flask and freeze-thawed three times in the vacuum line. Potassium *tert*-butyloxide (1 M in THF, 25 uL, 25 umol) was added *via* microliter syringe under nitrogen atmosphere, THF was then removed by vacuum. 1, 2-butylene oxide (BO) monomers (~0.6 mL) were stirred with freshly crushed calcium hydride over 24 h. After degassed in the vacuum line, they were distilled under reduced pressure into another flask that contained dibutylmagnesium. BO monomers were then immediately distilled into the reactor flask. Toluene was distilled into the reactor flask in the vacuum line. The weight ratio of monomer to solvent varied from 1:1 to 1:3, and the molar ratio of initiator to 18-crown-6 was 1:1. The reaction temperature was maintained at 0 °C. The copolymers in different compositions were obtained by taking an aliquot at a particular time during the polymerization, which was then terminated with methanol and precipitated into methanol several times, and dried for use.

### Synthesis of diblock copolymers

The synthesis of diblock copolymers is similar to that of gradient copolymers except that BO monomers were added after polymerization of liquid crystalline monomers completed. Briefly, a high vacuum reactor flask containing a stir bar was placed in the high vacuum line and flame-dried. The liquid crystalline monomers (0.5 g, 1.34 mmol) were added into the flask, and dried at 40 °C for 2 h. 18-crown-6 (14 mg, 50 umoL) and potassium *tert*-butoxide (1 M in THF, 25 uL, 25 umol) were added under the nitrogen atmosphere and THF was then removed in vacuum. Toluene was distilled into the reactor flask and the reaction was maintained at 0 °C for 7 days. BO monomers (~0.6 mL) were stirred with freshly crushed calcium hydride over 24 h. After degassed in the vacuum line, they were distilled under reduced pressure into another flask that contained dibutylmagnesium. They were then immediately distilled into the reactor flask. The reaction was conducted at 0 °C. The block copolymers with different lengths of PBO block were obtained by taking an aliquot at a particular time during the polymerization. They were then terminated with methanol and precipitated into methanol several times and dried for use.

### Characterization methods

$^1$H NMR spectra were recorded on a Varian MERCURY spectrometer (400 MHz) using $CDCl_3$ as the solvent. The molecular weights of the polymers were characterized by gel permeation chromatography (Wyatt Dawn EOS) with a multi-angle light scattering detector. THF was used as the eluent. The polydispersity index (PDI = $M_w/M_n$) was obtained accordingly. The investigation of thermal behavior was performed on a differential scanning calorimeter (Perkin Elmer DSC 8500). A cooling process from isotropic melt was always carried out first; subsequent heating was performed at a scanning rate equal to the previous cooling process.

Two-dimensional (2D) SAXS experiments were carried out on the synchrotron X-ray beam line BL16B1 in Shanghai Synchrotron Radiation Facility (SSRF). The wavelength of the X-ray beam is 1.239 Å. The scattering vector q ($q = 4\pi\sin\theta/\lambda$, where $\lambda$ is the X-ray wavelength and $2\theta$ is the scattering angle.) is calibrated using silver behenate. A Linkam heating stage with $N_2$ protection environment and a MarCCD detector were used. 2D WAXS measurements were conducted on the synchrotron X-ray beam line BL14B1 in SSRF. In temperature dependent X-ray scattering experiments, the sample was always isothermally stabilized at preset temperature for 15 min before starting the measurement.

## Results and discussion

### Chemical structure characterization of copolymers

The chemical structures of the copolymers have been fully characterized by $^1$H NMR. The $^1$H NMR spectra of copolymers which have been continuously taken out of the reactor during polymerization process are shown in Supporting Information (Fig. S2) and a representative spectrum is demonstrated in Fig. 1. The molecular weights and the compositions of the

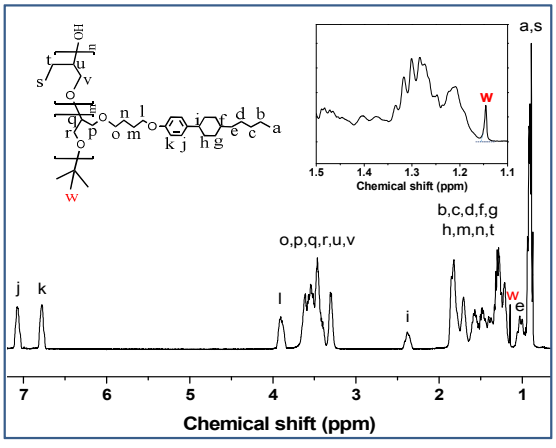


**Fig. 1** Representative $^1$H NMR spectrum of $E_{35}$-*g*-$B_{34}$ in $CDCl_3$. Inset is the enlarged chemical shift regime where the terminal group can be clearly identified.

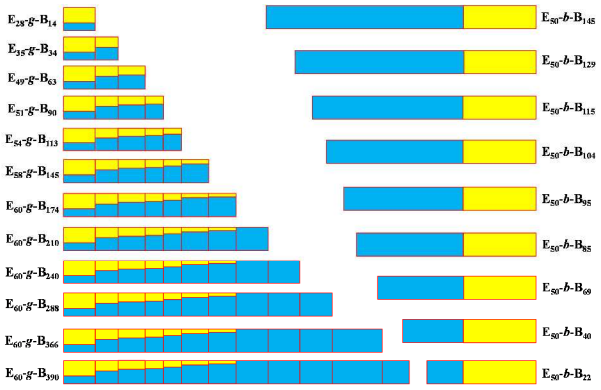


**Fig. 2** Schematic illustration of composition profiles of the gradient copolymers $E_m$-*g*-$B_n$ and block copolymers $E_m$-*b*-$B_n$. The area of yellow block represents the molar fraction of E and the area of blue block represents that of B at each step of polymerization process.

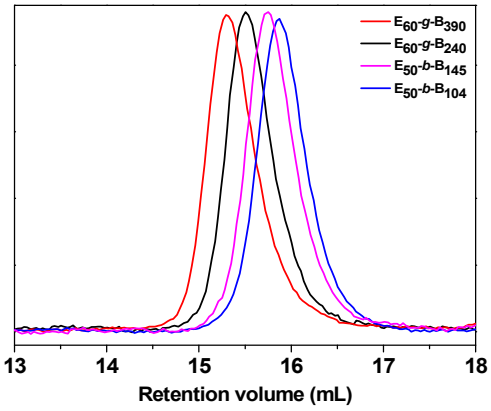


**Fig. 3** Representative GPC-RI chromatograms of $E_{60}$-*g*-$B_{240}$ (PDI = 1.01), $E_{60}$-*g*-$B_{390}$ (PDI = 1.01), $E_{50}$-*b*-$B_{104}$ (PDI = 1.01) and $E_{50}$-*b*-$B_{145}$ (PDI = 1.01). Their molecular weights based on $^1$H HMR measurements are 39.8 kg/mol, 50.6 kg/mol, 26.2 kg/mol and 29.2 kg/mol, respectively.

copolymers are determined by the integrals of resonances ascribed to aromatic protons (δ = 6.78 ppm and 7.08 ppm) in the mesogenic units and aliphatic protons with chemical shifts between 3.2 ppm and 3.75 ppm. They are further compared with the resonance of *tert*-butyl end group, as shown in the inset of Fig. 1. It is found that anionic ring-opening copolymerization of liquid crystalline epoxy monomers and BO monomers in a batch mode can offer a facile way to synthesize gradient copolymers with controlled monomeric sequences. With a sequential addition of monomers, block copolymers can be also obtained, which will be studied in comparison with the gradient copolymers. The gradient copolymers are denoted as $E_m$-*g*-$B_n$, and the block copolymers are denoted as $E_m$-*b*-$B_n$, where E represents the liquid crystalline units EOBC[35-37] and B represents BO units, m and n are the mean numbers (nominal values) of the units, respectively, which are estimated on the basis of $^1$H NMR results with the error less than 2%.

The evolution of the composition profiles is schematically demonstrated in Fig. 2. As shown in the figure, the gradient copolymers are obtained at the early stages of the copolymerization process. With the growth of the chain, the gradient length builds up gradually. The obtained gradient copolymer of the highest molecular weight is $E_{60}$-*g*-$B_{174}$ (E% ~ 64.1 in volume fraction). Then pure PBO block continuously grows and the so-called tapered-block copolymers form. The cumulative molar fraction of the liquid crystalline units as a function of the normalized chain length is also shown in Fig. S3. In contrast, the block copolymers have a fixed length of liquid crystalline block and a continuous growth of the PBO blocks. The compositions of the chains at each growth step enable us to further explore the relationships between the chemical compositions and physical properties accordingly.

Representative GPC-RI chromatograms of the gradient and block copolymers are shown in Fig. 3 as examples. The symmetric mono-model peaks at different retention volumes give rise to very narrow polydispersities (PDI ~ 1.01), indicating a success in the anionic polymerization throughout the whole process. They shift to smaller retention volumes with increase of the molecular weights. It is worth noting that the monodispersity of molecular weight distribution is important to the study of the gradient liquid crystalline copolymers. Otherwise, the influence of the polydispersity on the liquid crystalline phase behavior could be substantial.[38, 39]

In order to obtain the insights into the copolymerization process, the consumption of monomers at each stage of the copolymerization has been followed directly by using in situ NMR technique.[43, 44] The detailed synthetic procedure and analysis are described in the Supporting Information. The normalized amount of unreacted monomer is plotted *vs* total conversion, as shown in Fig. S6. The concentration of monomer E decreases more rapidly than that of B monomer in the reaction mixture before ~80% E was consumed, indicating that monomer E is incorporated faster compared to monomer B. These results are consistent with the compositional drift observed in the copolymers previously, where the liquid crystalline units were consumed early in the copolymerization and a gradient composition profile was resulted. It is worth noting that the liquid crystalline unit has a larger side group and consequently is sterically hindered in comparison to the BO monomer, while it has a higher reactivity. We think that this might be attributed to the different chemistries in the side groups of these two monomers in light of recent research on the copolymerization of epoxides.[45] In their work, it was found that the relative epoxide comonomer reactivities were determined primarily by the relative tendency of the epoxide monomer to coordinate with the potassium counter-ion. Therefore, we conjecture that the ether substituent side group in the liquid crystalline units might facilitate this process and consequently leads to the higher reactivity than that of the BO monomers with only alkyl substituent (ethyl group), which might also result in the penultimate effect.

### Thermal analysis of the copolymers

For gradient copolymers, smooth variations of the compositions along the chains are expected to result in unique thermal properties.[19, 40, 41] The glass transition temperatures (Tg) of the gradient copolymers are found different from those of the nanophase separated diblock copolymer counterparts as well as the random copolymers possessing no composition gradient in their average compositions. For random copolymers, a single Tg is usually observed.[41] For phase separated diblock copolymers, typically two Tgs can be observed.[3, 40, 41] In our liquid crystalline block copolymers, at least one glass transition around 0 °C is discernible, ascribed to that of the liquid crystalline block E.[36] The glass transition of the PBO block should be around -70 °C according to the literature,[46] which overlaps with the upturn of the DSC curve at low temperature regime in Fig. 4a. Nevertheless, it might be still discernible in

the block copolymers with higher PBO contents (as illustrated in Fig. S7). In contrast, the gradient copolymers exhibit broad glass transition temperature regions. With increase of the gradient length, the breadth of the Tg region becomes broader. The high-temperature end of the Tg remains nearly constant although still lower than that of the liquid crystalline homopolymer, the low-temperature end shifts towards that of the PBO homopolymer. This is understandable since the BO content increases with the growth of the chains. The increase of breadth of the Tg with the gradient length should be the direct consequence of the gradient composition change along the chains, which provides an extremely heterogeneous environment for the segmental dynamics.[47] When the gradient length increases further into the tapered-block copolymer regime, the breadth of Tg keeps almost constant. This can be ascribed to the fact that only pure BO units are added to the gradient portion in this case.

Another distinct feature in the thermal behaviors of these gradient and block copolymers lies in the liquid crystalline phase transformation. The DSC thermograms of the block copolymers show a dominant thermal transition at ~112 °C in Fig. 4a, which is ascribed to the transition from the liquid crystalline SmA phase to the isotropic melt of the EOBC block, although it is less sharper than that of the EOBC homopolymer.[36] A weak transition from the HexB phase to the SmA phase at ~45 °C, where the packing of mesogens within the liquid crystalline layers changes from hexagonal[48] to fluidic state, is also discernible in the diblock copolymers. In dramatic contrast, the gradient copolymer generally exhibits a very broad liquid crystalline phase transition. For the gradient copolymers of short gradient lengths, $E_{28}$-*g*-$B_{14}$ and $E_{35}$-*g*-$B_{34}$, the phase transitions are more obvious as shown in the first two DSC curves on the bottom of Fig. 4b. This is due to their relatively high contents of the liquid crystalline units, which are 67% and 51% in molar fraction, respectively. However, they are still much broader than those of the block copolymers, and the transition temperatures are apparently lower as well. With further increase of the gradient length, the transition appears much weaker due to the increase of the BO fraction. Nevertheless, the thermal transition remains when the molar faction of liquid crystalline units reaches 26% ($E_{60}$-*g*-$B_{174}$), and thereafter a pure PBO block continues to grow. For the liquid crystalline random copolymer, the liquid crystalline phase behavior can be retained even the molar fraction of mesogenic units is as low as 9%.[49] Although the thermal transformations of the gradient copolymers sometimes are barely discernible in the DSC measurements, the formation of liquid crystalline phases and their transformations are confirmed by the following X-ray scattering experiments. It is thus clear that the sequence distribution of the gradient copolymers has a dramatic effect on their thermal phase behaviors. However, thermal analysis cannot provide detailed structure information. In order to relate the thermal phase behaviors to the corresponding structures and to reveal how the distribution of BO units in the backbones affect the liquid crystalline phase structures and the resulting nanophase structures, SAXS and WAXS experiments are carried out as illustrated in the next section.

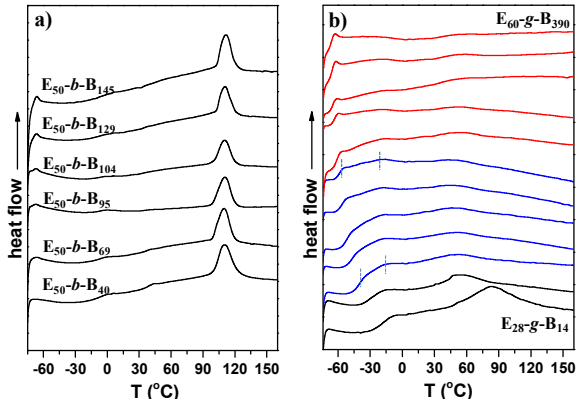


**Fig. 4** DSC second heating curves of (a) the block copolymers and (b) the gradient copolymers at a scanning rate of 20 °C/min. From the bottom to the top in (b), the gradient copolymer shown in Fig. 2. The red curves fall into the tapered-block copolymer regime. The vertical dot lines mark the glass transition regions.

### Structure characterization of the copolymers

Fig. 5 shows 1D SAXS profiles of the gradient copolymers with growth of the polymer chains. As illustrated in the profiles of $E_{28}$-*g*-$B_{14}$ and $E_{35}$-*g*-$B_{34}$ samples in the bottom of the figure, there solely appears a diffraction peak at q ~ 1.38 $nm^{-1}$, which results from the reflection of layered liquid crystalline structure. As the gradient length further increases, for example, to $E_{49}$-*g*-$B_{63}$, a distinct peak located at q ~ 0.53 $nm^{-1}$ emerges, indicating the occurrence of phase separation. Most of the samples exhibit a single scattering peak at low angle region, indicative of a limited ordering of the nanophase separated structure which is usually the case for gradient copolymers.[50] Nonetheless, weak higher-order peaks from nanophase separated structure in some copolymers can still be observed, as demonstrated more obviously in the following. It is also found that once the nanophase separated structure forms, the diffraction peak originating from the liquid crystalline layers becomes broader and apparently asymmetric, in contrast with those of $E_{28}$-*g*-$B_{14}$ and $E_{35}$-*g*-$B_{34}$ possessing the shortest gradient lengths, where no phase separation can be observed and the diffraction peaks from the liquid crystalline layers are narrow and symmetric.

In layered liquid crystalline phase, phase separation between the backbones and the mesogenic groups takes place, where the

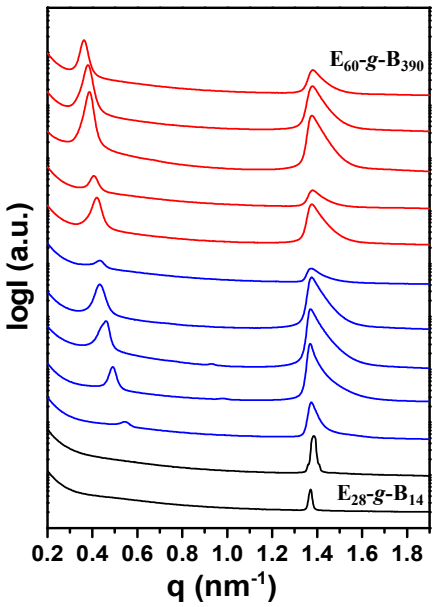


**Fig. 5** 1D SAXS profiles of the gradient copolymers. From the bottom to the top, the compositions of the gradient copolymers correspond to those in Fig. 2.

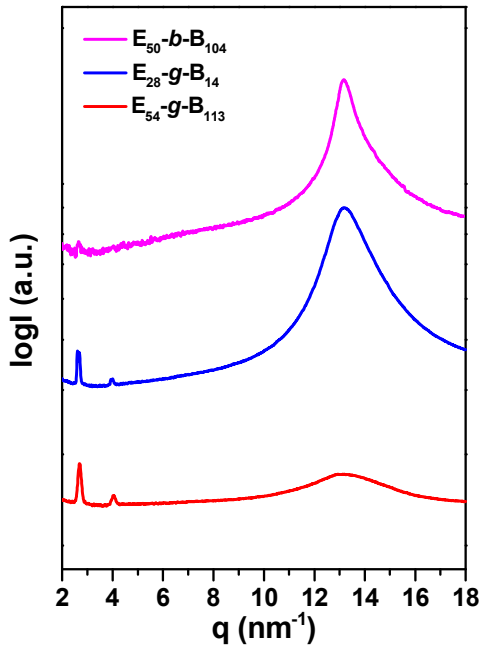


**Fig. 6** 1D WAXS profiles of the block copolymer and the gradient copolymers.

backbones are constrained in-between the liquid crystalline layers.[33, 34] In liquid crystalline gradient copolymers, the non-mesogenic BO units have to be accommodated in-between the liquid crystalline layers. The gradual increase of the amount of BO units along the chain inevitably results in swelling of the backbone region. This is consistent with the fact that the thickness of liquid crystalline layers is generally larger than that of homopolymers. It is worth noting that once the gradient length is above that of $E_{35}$-*g*-$B_{34}$, a much broader asymmetric reflection peak from liquid crystalline layers is observed in contrast with that of homopolymer[35, 36] and block copolymers as shown below. This suggests a thickness distribution of liquid crystalline layers. The broadening of reflection peak in the wide-angle side may indicate a coexistence of liquid crystalline layers in a smaller thickness. This phenomenon cannot result from the tilting of mesogens since no such behavior has been observed, as elucidated in the 2D WAXS pattern in Fig. S9. This could be related to increased extent of interdigitation of the mesogens, considering the tendency to expand the mesogens' packing with incorporation of BO units between the mesogens along the chain. As shown in the WAXS profiles of copolymers in Fig. 6, the block copolymer exhibits a sharp reflection peak characteristic of the hexagonal close packing of mesogens, while the gradient copolymer $E_{28}$-*g*-$B_{14}$ with a small content of BO units already shows the broadening of the reflection peak. Further increase of content of BO unit, *e.g.* in $E_{54}$-*g*-$B_{113}$, leads to a broad halo characteristic of disordered packing, which facilitates self-organization of mesogens into partial interdigitation state.Nanophase separation into ordered structures has been observed in the liquid crystalline gradient copolymers with increased gradient lengths. As shown in Fig. 7a for typical examples, $E_{54}$-*g*-$B_{113}$ shows a mixed structure at low temperature, where the q values marked with thin black arrows are 0.44 $nm^{-1}$ and 0.76 $nm^{-1}$ at a ratio of 1:√3, indicating a hexagonal packed cylinders (HPC) structure. While those marked with red arrows are 0.46 $nm^{-1}$ and 0.93 $nm^{-1}$ at a ratio of 1:2, belonging to a lamellae (Lam) structure. This mixed nanophase separated structure eventually evolves into a Lam structure above 60 °C. For $E_{60}$-*g*-$B_{288}$ (Fig. 7b), the q values at 0.39 $nm^{-1}$ and 0.67 $nm^{-1}$ at a ratio of 1:√3 suggests a HPC structure. For block copolymer $E_{50}$-*b*-$B_{104}$ as an example (Fig. 7c), besides the reflection peak belonging to liquid crystalline layers located at q ~ 1.38 $nm^{-1}$, the rest reflection peaks marked with arrows are located at q ~ 0.51 $nm^{-1}$, 0.89 $nm^{-1}$, 1.02 $nm^{-1}$, 1.48 $nm^{-1}$ and 1.69 $nm^{-1}$ at 80 °C at a ratio of 1:√3:√4:√9:√11. This indicates the formation of a well-ordered HPC structure, as also elucidated in 2D SAXS pattern in Fig. S8.

The gradient copolymers and the block copolymers are found to show different evolutions of the nanophase separated structures with temperature, as shown in Fig. 7, where temperature dependent 1D SAXS profiles of $E_{54}$-*g*-$B_{113}$, $E_{60}$-*g*-$B_{288}$ and $E_{50}$-*b*-$B_{104}$ are compared. It notes that $E_{54}$-*g*-$B_{113}$ and $E_{50}$-*b*-$B_{104}$ have similar molecular weights and average compositions; $E_{60}$-*g*-$B_{288}$ is a tapered-block copolymer. The plots of q values of the first reflection peak from the nanophase separated structure (among the peaks marked with red arrows) reveal that the temperature dependence of their domain sizes follow different trends, as shown in Fig. 8a. The domain sizes of the gradient copolymers increase with increase of temperature, in contrast, the domain size of the block copolymer decreases with increase of temperature. Moreover, gradual loss of liquid crystalline order is observed in the gradient copolymers, while it is abrupt in the block copolymer. It is worth mentioning that the reflection peak from liquid crystalline layers in the block copolymer is narrow and symmetric in comparison with the broad and asymmetric peak in the gradient copolymers. In $E_{50}$-*b*-$B_{104}$, the isotropization of liquid crystalline block coincides with the order-to-disorder transition (ODT) of the block copolymer, as shown in the plot of reverse intensity of the first reflection peak $I^{-1}$ *vs* $T^{-1}$ in Fig. 8b. This suggests a liquid crystallization induced phase separation process. In the gradient copolymers, the gradual incorporation of non-mesogenic BO units between the

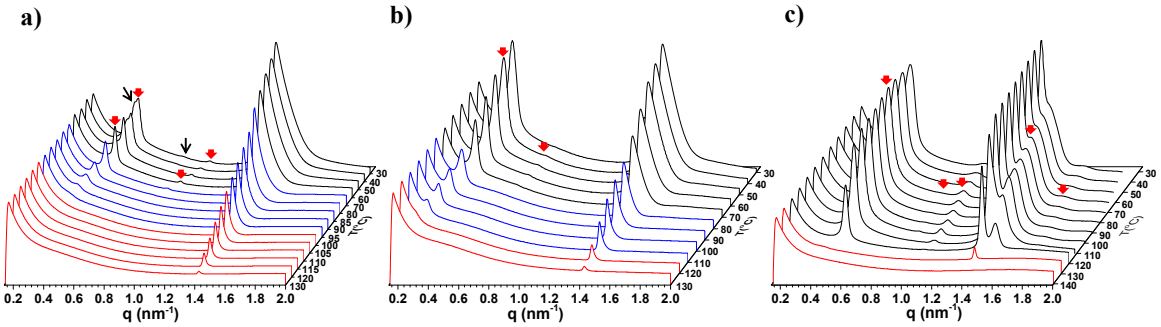


**Fig. 7** Temperature dependent 1D SAXS profiles of $E_{54}$-*g*-$B_{113}$ (a), $E_{60}$-*g*-$B_{288}$ (b), and $E_{50}$-*b*-$B_{104}$ (c).

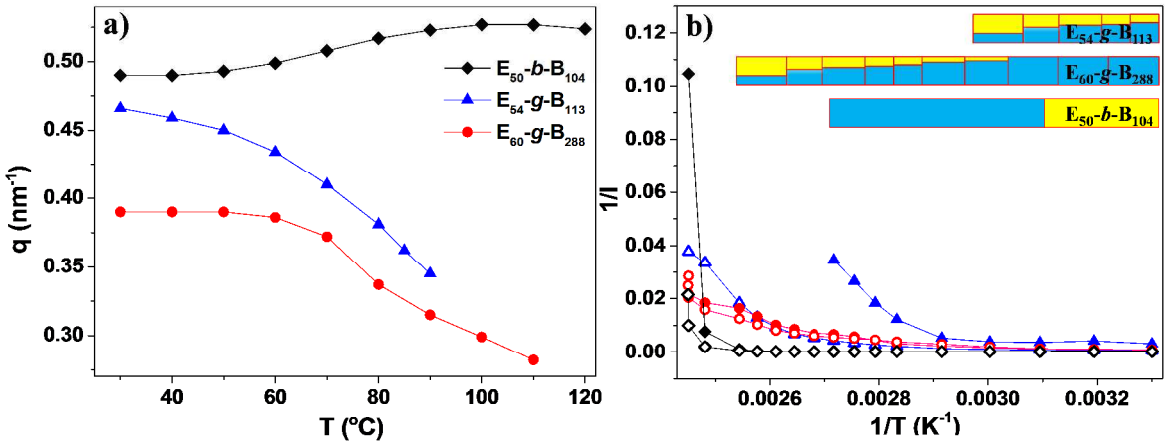


**Fig. 8** Evolution of q value of the first reflection peak from the nanophase separated structures of $E_{50}$-*b*-$B_{104}$, $E_{54}$-*g*-$B_{113}$ and $E_{60}$-*g*-$B_{288}$ with temperature as discussed in the text (a) and its reverse intensity $I^{-1}$ *vs* $T^{-1}$ (solid symbols) in comparison with the reverse intensity of reflection from liquid crystalline layers (hollow symbols) $I^{-1}$ *vs* $T^{-1}$ (b).

mesogens would lead to a broad distribution of phase stability. The liquid crystalline domains of poorer stability would melt first, which should start from BO rich parts in the gradient chains. Therefore, progressive melting of liquid crystalline phase and continuous re-organization of the system into a new phase separated structure take place with increase of temperature. The increase of *d*-spacing of the nanophase separated structures of the gradient copolymers with temperature is understandable considering the decrease of density upon melting of liquid crystalline phases.[51] In the block copolymer, the liquid crystallinity remains constant till the liquid crystalline phase melts. It is also found that the ODT of $E_{54}$-*g*-$B_{113}$ takes place before the complete melting of liquid crystalline phase, while the nanophase separated structure of the tapered-block copolymer $E_{60}$-*g*-$B_{288}$ remains until the liquid crystalline phase melts. This suggests that a small liquid crystalline content in the system is enough to induce the phase separation of the tapered-block copolymer, which has an increased chain length with an additional pure PBO block compared with the gradient copolymer.

Gradient copolymer turns out to be a highly heterogeneous system. There always exists a high degree of mixing between the component units and a broad interface in the case of phase separation. This work reveals that the gradient composition of the liquid crystalline copolymer endows a large heterogeneity in the liquid crystalline phase size and stability through the constrained backbones in-between the liquid crystalline layers. This is reflected by the extremely broad liquid crystalline phase transformation region in calorimetric measurements. As also elucidated by X-ray scattering experiments, the mesogenic packing becomes disordered with increase of gradient length and a thickness distribution of the liquid crystalline layers is resulted. Consequently, this leads to a progressive melting of the liquid crystalline phases with temperature and a distinct structure evolution in contrast with the block copolymer. The gradient nature in chain architecture imparts an extreme heterogeneity in segmental dynamics as well. A dramatically broad glass transition is observed in the liquid crystalline gradient copolymers which breadth increases with the gradient length. It is actually surprising to observe nanophase separation in liquid crystalline gradient copolymers. Phase separation in gradient copolymers is predicted to be more difficult than diblock copolymers. According to self-consistent mean-field theory, the symmetric gradient copolymers exhibit a sinusoidal composition profile and a broad interface in contrast to a square wave composition profile in ordered block copolymers.[9] For symmetrical gradient copolymer, the critical $\chi N$ for ODT is 29.25 in contrast to 10.495 for diblock copolymer, where $\chi$ is the Flory-Huggins interaction parameter and N is the degree of polymerization.[8] This is consistent with the observation of different orderings of the phase separated structures between the liquid crystalline gradient copolymers and the block copolymers above. The nanophase separation in the liquid crystalline gradient copolymer would thus generate one phase rich in BO units and another poor along the backbones, which are constrained in-between the liquid crystalline layers. The phase separation tendency along the backbone seems not averaged out by the surrounding liquid crystalline field. Phase separation in side-chain liquid crystalline block copolymers is actually much more sophisticated than coil-coil diblock copolymers, which arises from the interplay between block copolymer nanophase separation and the orientational ordering of liquid crystalline units. The contribution to the interaction parameter may need to take into account interactions between all components in the system, including backbone blocks and incompatible mesogens attached to them.[52] Nevertheless, the phase separation of the gradient backbones turns out to make a critical contribution. The nanophase separation in the liquid crystalline gradient copolymers driven by the compositional ordering of the confined backbones represents an interesting experimental observation which deserves further theoretical work.

## Conclusions

Liquid crystalline gradient polyethers with narrow molecular weight distributions have been successfully synthesized in a batch approach in the course of living anionic ring-opening copolymerization. The compositional sequence patterns of the copolymers have been identified at various chain growth stages. The thermal behaviors and phase structures of the gradient copolymers in different compositions have been investigated, revealing distinct behaviors in comparison with the block copolymer counterparts obtained through the sequential anionic polymerization. The intrinsic heterogeneity existed in the gradient copolymers coupled with the liquid crystalline functionality imparts a broad glass transformation, phase stabilities, and unique evolution of the nanophase separated



 

structures. This work demonstrates that the sequence control over the chain architectures to obtain structural gradient multi-component copolymers is an efficient way to tune structures and properties which are not attainable by block or random copolymers. This approach could ultimately develop materials with superior performance different from the conventional design based on uniformity.[53]

## Acknowledgements

We appreciate BL14B and BL16B beam lines in SSRF. Research is supported by the NSFC (No. 21074070) and NCET-11-0335.

## Notes and references

*Department of Polymer Science, School of Chemistry and Chemical Engineering, Shanghai Jiao Tong University, Shanghai, 200240, P. R. China. E-mail addresses: hmxiong@sjtu.edu.cn; Tel.: 86-21-34202544.*

† Electronic Supplementary Information (ESI) available: synthetic routes, $^1$H NMR spectra of gradient copolymers, cumulative molar fractions of components of gradient copolymers as a function of normalized chain length, in situ $^1$H NMR spectra, residual monomer concentrations as a function of total conversion, DSC of $E_{50}$-*b*-$B_{145}$, 2D SAXS and WAXS patterns of $E_{50}$-*b*-$B_{104}$, 2D WAXS pattern and azimuthal scans of $E_{54}$-*g*-$B_{113}$. See DOI: 10.1039/b000000x/

1 G. Odian, *Principles of Polymerization*, John Wiley & Sons, Inc.: Hoboken, New Jersey, 2004, Ch. 6.
2 F. S. Bates, G. H. Fredrickson, *Annu. Rev. Phys. Chem.*, 1990, **41**, 525.
3 I. W. Hamley, *The Physics of Block Copolymers*, Oxford University Press: Oxford, U.K., 1998.
4 T. Pakula, K. Matyjaszewski, *Macromol. Theory Simul.*, 1996, **5**, 987.
5 A. Aksimentiev, R. Holyst, *J. Chem. Phys*., 1999, **111**, 2329.
6 K. R. Shull, *Macromolecules*, 2002, **35**, 8631.
7 G. T. Pickett, *J. Chem. Phys*., 2003, **118**, 3898.
8 M. D. Lefebvre, M. Olvera de la Cruz, K. R. Shull, *Macromolecules*, 2004, **37**, 1118.
9 R. Jiang, Q. H. Jin, B. H. Li, D. T. Ding, R. A. Wickham, A. C. Shi, *Macromolecules*, 2008, **41**, 5457.
10 N. B. Tito, S. T. Milner, J. E. G. Lipson, *Macromolecules*, 2010, **43**, 10612.
11 V. Ganesan, N. A. Kumar, V. Pryamitsyn, *Macromolecules*, 2012, **45**, 6281.
12 T. Hashimoto, Y. Tsukahara, K. Tachi, H. Kawai, *Macromolecules*, 1983, **16**, 648.
13 Y. Tsukahara, N. Nakamura, T. Hashimoto, H. Kawai, T. Nagaya, Y. Sugimura, S. Tsuge, *Polym. J.*, 1980, **12**, 455.
14 S. Jouenne, J. A. Gonzalez-Leon, A. V. Ruzette, P. Lodefier, S. Tence-Girault, L. Leibler, *Macromolecules*, 2007, **40**, 2432.
15 N. Singh, M. S. Tureau, T. H. Epps, *Soft Matter,* 2009, **5**, 4757.
16 R. Roy, J. K. Park, W.-S. Young, S. E. Mastroianni, M. S. Tureau, T. H. Epps, *Macromolecules*, 2011, **44**, 3910.
17 J. R. Brown, S. W. Sides, L. M. Hall, *ACS Macro Lett.*, 2013, **2**, 1105.
18 K. Matyjaszewski, M. J. Ziegler, S. V. Arehar, *J. Phys. Org. Chem.*, 2000, **13**, 775.
19 D. Neugebauer, M. Theis, T. Pakula, G. Wegner, K. Matyjaszewski, *Macromolecules*, 2006, **39**, 584.
20 K. Matyjaszewski, N. V. Tsarevsky, *J. Am. Chem. Soc.*, 2014, **136**, 6513.
21 D. Benoit, C. J. Hawker, E. E. Huang, Z. Q. Lin, T. P. Russell, *Macromolecules*, 2000, **33**, 1505.
22 M. Gray, H. Zhou, S. T. Nguyen, J. M. Torkelson, *Macromolecules*, 2004, **37**, 5586.
23 M. M. Mok, J. Kim, J. M. Torkelson, *J. Polym. Sci., Part B*, 2008, **46**, 48.
24 J. Kim, M. K. Gray, H. Y. Zhou, S. T. Nguyen, J. M. Torkelson, *Macromolecules*, 2005, **38**, 1037.
25 P. Hodrokoukes, G. Floudas, S. Pispas, N. Hadjichristidis, *Macromolecules*, 2001, **34**, 650.
26 K. Karaky, E. Pere, C. Pouchan, J. Desbrieres, C. Derail, L. Billon, *Soft Matter*, 2006, **2**, 770.
27 U. Beginn, *Colloid Polym. Sci.*, 2008, **286**, 1465.
28 A. Natalello, A. Alkan, P. von Tiedemann, F. R. Wurm, H. Frey, *ACS Macro Lett.*, 2014, **3**, 560.
29 K. Knoll, N. Niessner, *Macromol. Symp.*, 1998, **132**, 231.
30 X. Y. Sun, Y. W. Luo, R. Wang, B. G. Li, B. Liu, S. P. Zhu, *Macromolecules*, 2007, **40**, 849.
31 V. S. Reuss, M. Werre, H. Frey, *Macromol. Rapid Commun.*, 2012, **33**, 1556.
32 W. Zhang, J. Allgaier, R. Zorn, *Macromolecules*, 2013, **46**, 3931.
33 V. Percec, C. Pugh, *Side Chain Liquid Crystal Polymers*, ed. C. B. McArdle, Blackie and Sons: Glasgow, 1989, Ch. 3.
34 D. Demus, J. Goodby, G.W. Gray, H. W. Spiess, editors. *Handbook of liquid crystals*, WILEY-VCH Verlag GmbH, 1998, Ch. IV.
35 Y. Liu, Y. G. Li, H. M. Xiong, *ACS Macro Lett.*, 2013, **2**, 45.
36 Y. Liu, W. Wei, H. M. Xiong, *Polymer*, 2013, **54**, 6572.
37 W. Wei, Y. Liu, H. M. Xiong, *Polymer*, 2013, **54**, 6793.
38 T. Sagane, R. W. Lenz, *Polym. J.*, 1988, **20**, 923.
39 M. H. Li, P. Keller, E. Grelet, P. Auroy, *Macromol. Chem. Phys.*, 2002, **203**, 619.
40 A. I. Buzin, M. Pyda, P. Costanzo, K. Matyjaszewski, B. Wunderlich, *Polymer*, 2002, **43**, 5563.
41 C. L. H. Wong, J. Kim, J. M. Torkelson, *J. Polym. Sci. Part B: Polym. Phys.*, 2007, **45**, 2842.
42 J. Allgaier, S. Willbold, T. Chang, *Macromolecule*, 2007, **40**, 518.
43 B. Obermeier, F. Wurm, H. Frey, *Macromolecules* 2010, **43**, 2244.
44 W. Zhang, J. Allgaier, R. Zorn, *Macromolecules,* 2013, **46**, 3931.
45 B. F. Lee, M. Wolffs, K. T. Delaney, J. K. Sprafke, F. A. Leibfarth, C. J. Hawker, N. A. Lynd, *Macromolecules,* 2012, **45**, 3722.
46 J. Brandrup, E. H. Immergut, E. A. Grulke, *Polymer handbook, Fourth Edition,* John Wiley & Sons, 1998, Ch. 6, 214.
47 M. Z. Slimani, A. J. Moreno, G. Rossi, J. Colmenero, *Macromolecules*, 2013, **46**, 5066.
48 The 2D WAXS pattern of the block copolymer in Fig. S4 in Supporting Information illustrates the hexagonal packing of mesogens at room temperature.
49 H. Ringsdorf, A. Schneller, *Makromol. Chem. Rapid Commun.*, 1982, **3**, 557.
50 M. M. Mok, S. Pujari, W. R. Burghardt, C. M. Dettmer, S. T. Nguyen, C. J. Ellison, J. M. Torkelson, *Macromolecules*, 2008, **41**, 5818.

51 The density of EOBC homopolymer at room temperature is 0.99; the density of its melt at 140 ºC is 0.95, for example, which have been measured by a pycnometer.
52 I. I. Potemkin, A. S. Bodrova, *Macromolecules*, 2009, **42**, 2817.
53 J.-F. Lutz, *Polym. Chem.*, 2010, **1**, 55.